Intrinsic orbital and spin magnetism in Rh clusters on inert xenon matrices

V. Sessi, K. Kuhnke, J. Zhang, J. Honolka,* and K. Kern
Max-Planck-Institut für Festkörperforschung, Heisenbergstrasse 1, 70569 Stuttgart, Germany

C. Tieg
European Synchrotron Radiation Facility, BP 220, 38043 Grenoble Cedex 9, France

O. Šipr
Institute of Physics, ASCR, v.v.i., Cukrovarnicka, CZ-162 53 Prague, Czech Republic

J. Minár and H. Ebert
Department Chemie und Biochemie, Ludwig-Maximilians-Universität München, 81377 München, Germany

Intrinsic orbital and spin magnetic moments of quasifree Rh clusters on inert xenon buffer layers are measured using x-ray magnetic circular dichroism. The moments strongly vary as a function of average cluster size. A maximum total moment of 0.4 μ_B per atom and large orbital-to-spin moment ratios up to 60% appear for Rh_N clusters with average size $\bar{N} = 20$, suggesting that cluster geometries are biplanar. The magnetism is further studied between two extreme limits, from quasifree few-atom-sized clusters situated on a xenon layer toward Rh nanostructures in contact with a weakly interacting Ag(100) substrate. Density-functional theory calculations for different cluster sizes and Rh-Ag coordination explain the unexpected quenching of Rh moments in the case of directly deposited Rh on Ag(100) reported by Honolka *et al.* [Phys. Rev. B **76**, 144412 (2007)].

PACS number(s): 75.75.Cd, 61.46.Hk, 75.25.Dk

I. INTRODUCTION

Emerging magnetism in clusters of nonmagnetic bulk elements was observed in Stern-Gerlach experiments with Rh clusters of less than 100 atoms.[1] Strong oscillations of the total moment per atom are observed as a function of size in the smallest cluster size regime, which according to *ab initio* calculations can be attributed to finite-size effects in the electronic band structure. Theory predicts a fragile dependence of both the intrinsic orbital and spin moment formation on the structure and size of $4d$ and $5d$ metal clusters as well as large orbit-to-spin moment ratios due to the strong spin-orbit coupling effects, which can result in giant magnetocrystalline anisotropy effects.[2,3] Up to now experiments on free clusters were performed with access to the total moment per cluster only. However, the highly sensitive x-ray magnetic circular dichroism (XMCD) technique, in principle, allows to extract average orbital and spin moments separately, a challenging experiment which so far was realized only for $4d$ and $5d$ elements in contact with metal solids.[4–8]

In this work we present the use of inert xenon crystal matrices as an elegant way to study the moment formation in quasifree Rh_N metal clusters using XMCD. Cluster size-dependent spin- and orbital-moment contributions are separately determined using the sum rules[9,10] and are compared to calculations. The unique experiment allows us to confirm theoretical predictions of enhanced orbital-spin moment ratios in small free Rh clusters. We furthermore exploit the characteristic multistep buffer-layer-assisted growth (BLAG) process[11] to study coordination-dependent magnetism between two extremes, from quasifree few-atom Rh clusters (single atoms, dimers, trimers, etc.) on the inert xenon matrix

toward larger Rh structures in contact with a weakly interacting noble-metal substrate Ag(100). Our results suggest that the experimentally observed quenching of the moments during BLAG is mainly due to the increase in cluster size and not to cluster-substrate interactions. At the same time, we show that for Rh atoms deposited on Ag(100) without buffer layer, hybridization effects play a crucial role explaining the absence of moments in earlier measurements.[6]

II. EXPERIMENT

X-ray absorption spectra (XAS) were measured in the surface sensitive total electron yield (TEY) mode at the European Synchrotron Radiation Facility (beamline ID08). Rh $M_{3,2}$ absorption spectra μ^+/μ^- were measured at $T = 10$ K for positive/negative x-ray circular polarization with magnetic fields of up to $B = 5$ T applied parallel and antiparallel to the photon beam [see Fig. 1(a)]. For details on the sample preparation procedure and x-ray measuring geometry we refer the reader to Ref. 6. Xenon buffer layers of about 12 monolayers (ML) thickness were adsorbed on the clean Ag(100) substrate via a gas inlet system with the substrate held at temperatures $T = 10$ K. Thereafter, submonolayer amounts of Rh were evaporated at $T = 10$ K by means of an e-beam evaporator. The flux calibration and conversion to ML units were done by comparing the M_3 intensities with previous results in Ref. 6. In BLAG experiments the Xe layer was gradually desorbed by annealing the sample progressively from 10 K up to 150 K. During each step of BLAG the sample composition could be precisely monitored comparing the Ag $M_{5,4}$, Rh $M_{3,2}$, and Xe $M_{3,2}$ intensities. As shown in Fig. 1(b) at low Rh coverages the Rh $M_{3,2}$ absorp-
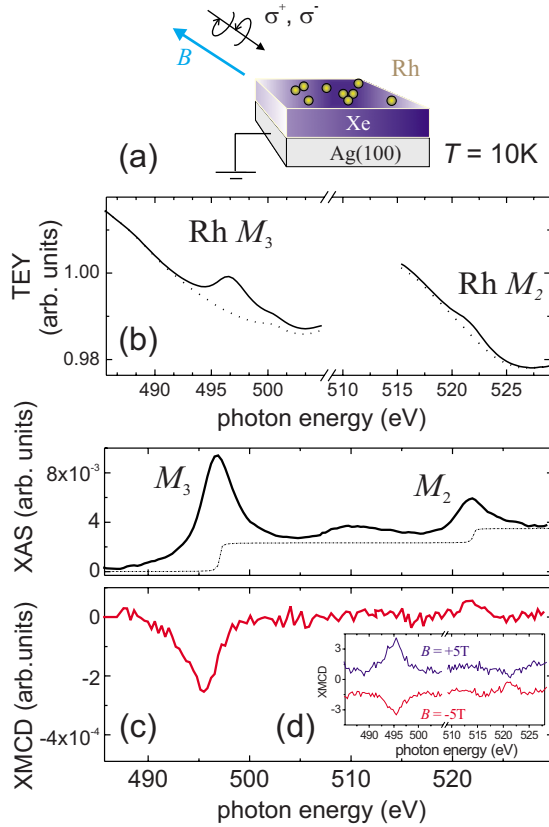
FIG. 1. (Color online) (a) Measurement setup. (b) Rh $M_{3,2}$ TEY spectra for (0.16 ± 0.05) ML Rhodium on xenon/Ag(100) ($T = 10$ K). The dotted line shows the xenon/Ag(100) background. (c) Background subtracted XAS and XMCD (d) XMCD spectra in opposite field polarities $B = \pm 5$ T.

FIG. 2. (Color online) (a) Calculated average effective spin (μ'_S) and orbital moment (μ_L) per hole and atom for different Rh coverages Θ. (b) Measured XMCD/XAS asymmetry evaluated at the M_3 edge (495 eV). (c) Orbital-to-spin moment ratios.

states at the Fermi level. All measured XMCD spectra show a pronounced peak at the M_3 edge while the M_2 peak is rather weak.

The asymmetry at the M_3 edge defined as the ratio between the XMCD and the XAS intensity allows for a rough estimation of the magnetic moment per Rh atom. As plotted in the inset of Fig. 2(a) the asymmetry is lowest at high coverages (1.2%) and nonmonotonously increases with decreasing coverage showing a maximum of 13.3% at about 0.1ML. According to Ref. 12 total moments of 1 μ_B per Rh atom produces a XMCD signal of about 13% with respect to the XAS intensity, which corresponds to average magnetic moments between 0.1 and 0.9 μ_B per atom in our measurements. These numbers are in reasonable agreement with Stern-Gerlach experiments, where the magnetic moment dropped from 0.8 μ_B to about 0.1 μ_B per atom when increasing the number atoms in the cluster from $N=9$ to $N=30$ atoms. As we will discuss later in this work, the appearance of a distinct maximum in the total moment with respect to cluster size is predicted by theory.

Orbital and spin magnetic moments and Rh $M_{3,2}$ XAS spectra were calculated *ab initio* for Rh systems with different Rh-Rh and Rh-Ag coordinations, relying on the relativistic impurity Green's function formalism (see Ref. 13 for more details). We have modeled on the one hand free, spherical-like Rh_{19} and Rh_{43} clusters corresponding to 2 and 3 coordination shells of bulk fcc Rh and on the other hand flat Rh structures such as a free-standing Rh monolayer, Rh monolayer on Ag(100), and flat Rh_4 clusters atop/within/below the Ag(100) surface. For Rh in contact with silver the Rh atoms were located in lattice sites of the underlying bulk fcc Ag lattice. Calculated magnetic moments and 4d-band holes n_h^d are given in Table I. Simulated XAS spectra are shown in Fig. 4(b).

Applying the XMCD sum rules[9,10] one can separately determine average orbital (μ_L) and effective spin (μ'_S) magnetic moments per Rh atom and 4d-band hole n_h^d from the experimental data. The XAS intensity is integrated across the resonances only (between 490–510 eV and 517–527 eV, respectively), avoiding the diffuse intensity between the resonant M_3 and M_2 edges. In Fig. 2(a) orbital and effective spin moments per hole obtained from the sum rules are plotted as

tion lines are superimposed by extended x-ray absorption fine structure oscillations originating from Ag $M_{5,4}$ and Xe $M_{3,2}$ absorption edges situated at lower energies. Hence, special care was taken to obtain high-quality background spectra of the Xe/Ag(100) systems before Rh deposition (dotted lines). To exclude unwanted time effects during the experiments we also made sure that there was no thermally induced change in the Xe-XAS during x-rays exposure. The residual nondichroic Rh XAS shown in Fig. 1(c) is defined as the background subtracted average $(\mu^+ + \mu^-)/2$ and the XMCD as $(\mu^+ - \mu^-)$. The XMCD spectra were recorded at highest available fields of $B = 5$ T and lowest temperatures of 10 K. Possible nonmagnetic artifacts in the XMCD were excluded by measuring the sign reversal of the XMCD upon changing the polarity of the magnetic field [see Fig. 1(d)].

III. RESULTS AND DISCUSSION

Using the procedure above, XAS and XMCD spectra were taken in the Rh coverage range $\Theta = 0.04 - 0.65$ ML with light at normal incidence. The typical Rh XAS shown in Fig. 1(c) exhibits prominent $M_{3,2}$ resonances separated by a diffuse intermediate peak around 510 eV typical for rhodium (see measured and calculated XAS spectra of bulk Rh in Fig. 4) and originating mostly from hybridized Rh 4p and 4d
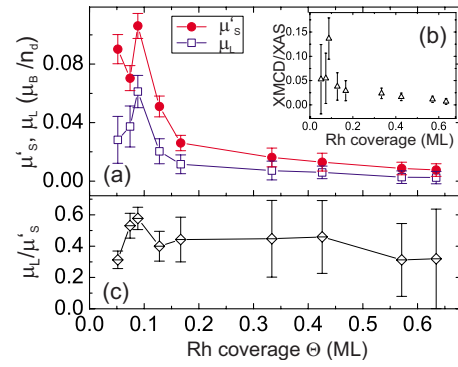
TABLE I. Average magnetic moments (in μ_B per atom) and d-band holes calculated for Rh in different geometries.

Geometry	μ_L	μ_S	μ_L/μ_S	$7\mu_T$	n_h^d
Rh ML free	0.204	1.194	0.17	−0.008	2.21
Rh ML supported	0.164	0.805	0.20	0.153	2.20
Rh4 atop	0.171	0.919	0.19	0.353	2.17
Rh4 surf. embedded	0	0		0	2.18
Rh4 buried	0	0		0	2.21
Rh19 free	0.102	0.771	0.13	−0.002	2.40
Rh43 free	0.010	0.210	0.05	0.013	2.44

a function of the Rh coverage Θ deposited on the xenon matrix. Increasing Θ leads to a rapid decay of both μ_L and μ_S' as expected for increasing average cluster sizes. The effective spin moment $\mu_S' = \mu_S + 7\mu_T$ includes a contribution from the magnetic dipole term μ_T, which is expected to be large in asymmetric bonding environments. Indeed, it follows from Table I that $7\mu_T$ is significant if Rh atoms are in direct contact with Ag(100) while it is negligible for pure Rh systems. Thus, for Rh situated on xenon μ_S' reflects to first approximation the spin moment μ_S. In the case of Rh deposited on a xenon matrix the comparison of the measured XAS line shape with simulated spectra in Fig. 4(b) indicates that clusters are decoupled from the Ag(100) substrate: only for the free Rh_N clusters and bulk rhodium the calculated XAS shows the characteristic diffuse peak observed in the experiment while for Rh coordinated to Ag atoms this peak significantly shifts to lower energies. As discussed above, for very low Rh coverages the moments shown in Fig. 2(a) do not change monotonously but exhibit a maximum at $\Theta \approx 0.2$ ML. If we assume $n_h^d = 2.4$ from Table I according to free Rh clusters, we can estimate total orbital (spin) moments of 0.15 μ_B(0.26 μ_B) per atom for $\Theta \approx 0.2$ ML, which gives total moments of 0.4 μ_B per atom, comparable to Stern-Gerlach experiments on Rh_N clusters of about $N = 20$.[1] Indeed, calculations predict a distinct maximum in the moment values for free nonicosahedral, biplanar Rh cluster geometries,[14] a cluster geometry which is reported to be energetically stable for late 3d and 4d metals.[15,16] Three kinds of biplanar growth sequences of Rh_N clusters show a peak in the total moment in the range $N = 10-15$ (Ref. 14) in fairly good agreement with our peak at $\bar{N} = 20$. Moreover, with calculated moment values below 1 μ_B per atom, biplanar clusters show lower moments than icosahedral clusters and fit much better to the experimental data.[17]

The complexity in the cluster moment formation is also visible in the ratio $r = \mu_L/\mu_S'$ between the orbital and effective spin moment plotted in Fig. 2(c), which is an excellent indicator of the relative strength of orbital magnetism independent of n_h^d. r shows oscillations at small coverages with values up to (0.6 ± 0.07) while at largest Θ it is reduced to 50%. So far r was only determined in Co-Rh and Fe-Rh compound nanoparticles where significantly smaller Rh values of 0.07 and 0.03–0.11 are reported, respectively.[18,19] While in these systems Rh moments are induced by adjacent magnetic 3d atoms, the magnetic properties of Rh clusters on

xenon presented in this work emerge purely from intrinsic Rh-Rh interactions. The enhanced intrinsic values μ_L/μ_S' are in agreement with Table I as well as with earlier calculations done for free Rh clusters.[20]

So far different amounts of Rh self-assembled on a frozen xenon layer during low-temperature molecular beam epitaxy have been studied in terms of moment formation. On the other hand keeping the coverage constant the cluster geometry can be altered by successively annealing the Xe buffer layer step by step: during this process Xe desorbs and clusters grow in size.[11,21] After each annealing step the temperature was reduced to $T = 10$ K to perform XMCD measurements. The XAS and XMCD signals of a 0.12 ML Rh/xenon system is shown in Figs. 3(a) and 3(b) for different annealing temperatures T_a. Between $T_a = 10$ and 150 K both the resonant $M_{3,2}$ absorption edges and the diffuse peak slightly shift by about 1 eV toward higher energies. The important effect, however, is visible in the XMCD signal, which is highly
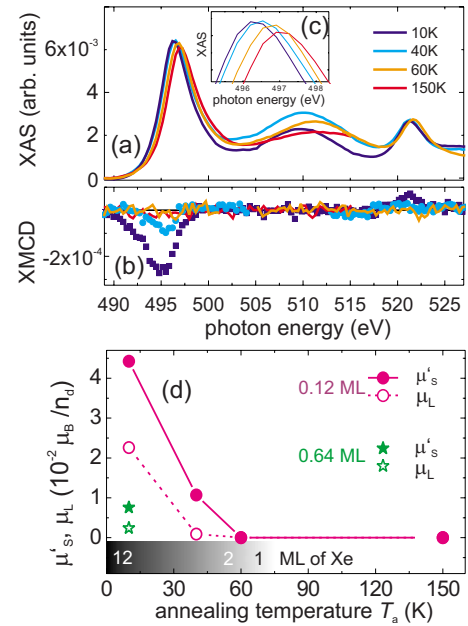

FIG. 3. (Color online) (a) XAS and (b) XMCD spectra for 0.12 ML Rh/Xe versus annealing temperature T_a. The inset (c) shows the peak at the M_3 edge, which shifts toward higher energies for increasing temperatures. (d) Extracted effective spin and orbital moments per hole and atom versus T_a.

susceptible to the annealing. In Fig. 3(d) the trend of effective spin and orbital moments per hole is shown as a function of the annealing temperature T_a. For comparison the values of the nonannealed sample with 0.65 ML is shown in the same graph. For $T_a = 40$ K both μ_L and μ'_S are strongly reduced but still finite; only for $T_a > 50$ K the dichroism is zero. In the lower part of the figure the desorption behavior of the Xe layer is schematically drawn for this range of temperature. At about 55 K we have desorption of the bulk Xe, however, 1–2 monolayers remain on the substrate. The residual Xe on the Ag(100) surface is desorbed when the temperature is further increased up to about 120 K. The measured moments are in line with what is expected from theory: μ_L and μ_S per atom in free Rh_N clusters (see Table I) are both strongly reduced when N is increased from 19 to 43. At $T_a > 50$ K finally the thermally induced growth of clusters seems to reach the threshold of average cluster sizes $N \approx 100$, where according to Cox *et al.* the moments disappear.

The combination of experiment and theory gives a thorough understanding of the magnetic-moment formation for Rh clusters prepared on a Xe matrix. In contrast directly deposited submonolayer amounts of Rh on Ag(100) at low temperatures were found to be nonmagnetic[6] while various theoretical calculations of different Rh cluster geometries predict sizable magnetism.[22–24] In the following we use again simulated spectra of Rh-Ag systems of different geometries to address this question. The measured XAS spectrum for 0.1 ML Rh directly deposited on Ag(100) shown in Fig. 4(a) is very different from the equivalent amount of Rh on xenon. In the former case the diffuse peak is absent and instead we observe a shoulder at the high-energy sides of the $M_{3,2}$ edges and a shift of the resonances to higher energies. Data not shown here prove that at higher coverages the diffuse peak is partially recovered, and the line shape approaches that of Rh bulk.[6] Such a behavior can be explained if we take into account alloying processes as modeled in the lower panel of Fig. 4(b), where we display calculated XAS spectra of a flat Rh_4 cluster located (i) on the Ag(100) surface "atop," (ii) incorporated into the surface layer "embedded," and (iii) incorporated into the subsurface layer "buried." In real samples a superposition of different geometries and cluster sizes would result in smearing-out of the shoulder at the high-energy side of the M_3 edge, yielding spectral shape similar to what was measured. According to Table I in this case the moments indeed vanish as observed in the experiments.

IV. CONCLUSIONS

In conclusion we monitored the formation of finite orbital and spin moments in Rh clusters decoupled by a xenon matrix. For small clusters of about 20 atoms in size total magnetic moments as large as 0.4 μ_B per atom are found, which decay with increasing cluster size. The purely intrinsic $4d$ metal magnetism shows drastically increased orbit-to-spin
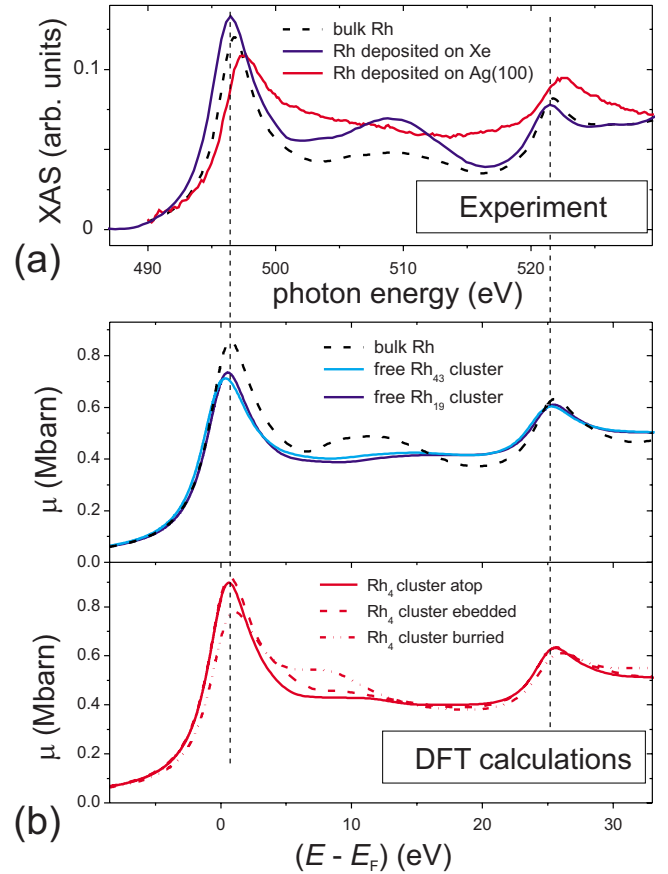

FIG. 4. (Color online) (a) Measured Rh $M_{3,2}$ XAS of Rh/xenon and Rh deposited on Ag(100) (from Ref. 6). For comparison bulk Rh is shown. (b) Calculated XAS spectra: (upper panel) free Rh_{43} and Rh_{19} clusters and bulk Rh, (lower panel) 2D Rh_4 clusters on top of Ag(100), embedded, and buried.

moment ratios compared to induced $4d$ moments measured in $3d$-$4d$ metal compounds. The experimental results together with density-functional theory calculations (i) suggest the cluster geometry to be biplanar in the free limit and (ii) explains the quenching of moments for Rh directly deposited on Ag(100) reported in Ref. 6. The approach of using xenon films for x-ray studies of electronic, magnetic, and structural properties under quasifree conditions is versatile and can be extended to various nano-objects such as multimetallic clusters, organic or even larger biological molecules. Regarding the determination of orbital moments of free magnetic clusters by XMCD we consider this approach unique at least until free-electron LASERs will be available.

*j.honolka@fkf.mpg.de

[1] A. J. Cox, J. G. Louderback, and L. A. Bloomfield, Phys. Rev. Lett. **71**, 923 (1993).

[2] Y. Mokrousov, G. Bihlmayer, S. Heinze, and S. Blügel, Phys. Rev. Lett. **96**, 147201 (2006).

[3] A. Smogunov, A. Dal Corso, A. Delin, R. Weht, and E. Tosatti, Nat. Nanotechnol. **3**, 22 (2008).

[4] G. R. Harp, S. S. P. Parkin, W. L. O'Brien, and B. P. Tonner, Phys. Rev. B **51**, 12037 (1995).

[5] J. Minár, S. Bornemann, S. Mankovsky, H. Ebert, M. Martins, M. Reif, L. Glaser, and W. Wurth, Phys. Status Solidi B **247**, 1180 (2010).

[6] J. Honolka, K. Kuhnke, L. Vitali, A. Enders, K. Kern, S. Gardonio, C. Carbone, S. R. Krishnakumar, P. Bencok, S. Stepanow, and P. Gambardella, Phys. Rev. B **76**, 144412 (2007).

[7] V. V. Krishnamurthy, N. Kawamura, M. Suzuki, T. Ishikawa, G. J. Mankey, P. Raj, A. Satyamoorthy, A. G. Joshi, and S. K. Malik, Phys. Rev. B **68**, 214413 (2003).

[8] N. Jaouen, F. Wilhelm, A. Rogalev, J. Goulon, J. M. Tonnerre, and S. Andrieu, J. Magn. Magn. Mater. **272-276**, E1615 (2004).

[9] P. Carra, B. T. Thole, M. Altarelli, and X. Wang, Phys. Rev. Lett. **70**, 694 (1993).

[10] B. T. Thole, P. Carra, F. Sette, and G. van der Laan, Phys. Rev. Lett. **68**, 1943 (1992).

[11] J. H. Weaver and G. D. Waddill, Science **251**, 1444 (1991).

[12] M. A. Tomaz, T. Lin, G. R. Harp, E. Hallin, T. K. Sham, and W. L. O'Brien, J. Vac. Sci. Technol. A **16**, 1359 (1998).

[13] O. Šipr, S. Bornemann, J. Minár, S. Polesya, V. Popescu, A. Šimůnek, and H. Ebert, J. Phys.: Condens. Matter **19**, 096203 (2007).

[14] F. Aguilera-Granja, J. M. Montejano-Carrizalez, and R. A. Guirado-López, Phys. Rev. B **73**, 115422 (2006).

[15] C. M. Chang and M. Y. Chou, Phys. Rev. Lett. **93**, 133401 (2004).

[16] Y.-C. Bae, H. Osanai, V. Kumar, and Y. Kawazoe, Phys. Rev. B **70**, 195413 (2004).

[17] Unlike the moments, our calculations show that the shape of the XAS of free clusters is little affected by the cluster geometry.

[18] M. Muñoz-Navia, J. Dorantes-Dávila, D. Zitoun, C. Amiens, B. Chaudret, M.-J. Casanove, P. Lecante, N. Jaouen, A. Rogalev, M. Respaud, and G. M. Pastor, Faraday Discuss. **138**, 181 (2008).

[19] A. Smekhova, D. Ciuculescu, P. Lecante, F. Wilhelm, C. Amiens, A. Rogalevand, and B. Chaudret, IEEE Trans. Magn. **44**, 2776 (2008).

[20] R. Guirado-López, P. Villaseñor-González, J. Dorantes-Dávila, and G. M. Pastor, J. Appl. Phys. **87**, 4906 (2000).

[21] V. Sessi, K. Kuhnke, J. Zhang, J. Honolka, K. Kern, A. Enders, P. Bencok, S. Bornemann, J. Minár, and H. Ebert, Phys. Rev. B **81**, 195403 (2010).

[22] V. S. Stepanyuk, W. Hergert, P. Rennert, K. Wildberger, R. Zeller, and P. H. Dederichs, Phys. Rev. B **59**, 1681 (1999).

[23] D. I. Bazhanov, W. Hergert, V. S. Stepanyuk, A. A. Katsnelson, P. Rennert, K. Kokko, and C. Demangeat, Phys. Rev. B **62**, 6415 (2000).

[24] S. Blügel, Phys. Rev. Lett. **68**, 851 (1992).